Journal of the Physical Society of Japan
Vol. 72, No. 5, May, 2003, pp. 1080–1086


# Total Electron Scattering Cross Sections for Simple Perfluorocarbons

Hiroyuki NISHIMURA*, Fumio NISHIMURA[1†], Yoshiharu NAKAMURA[2‡] and Keisuke OKUDA[2]

*Kasugai Branch of the Gaseous Electronics Institute, Kozoji, 1-13-11 Kasugai 4870033*
[1]*Research Laboratory for Nuclear Reactors, Tokyo Institute of Technology, Meguro-ku, Tokyo 1520033*
[2]*Department of Science and Technology, Keio University, Hiyosi, Yokohama 2238521*

(Received November 7, 2002)

Total electron scattering cross sections for $CF_4$, $C_2F_6$ and $C_3F_8$ have been measured in the energy range between 1.25 eV and 3000 eV using a compact linear transmission apparatus. Electrons scattered into a narrow forward angular range that should be counted in the scattered one were estimated utilizing measured quantities. The present results for $CF_4$ agree well with available data at low and high energies, while some discrepancies were seen at intermediate energies. Measured results for $C_2F_6$ and $C_3F_8$ were shown at high energies for the first time. Upper bound of the elastic cross sections for these molecules were estimated at electron energies higher than 20 eV.

KEYWORDS: electron scattering, electron molecule scattering, total cross section, perfluorocarbons
DOI: 10.1143/JPSJ.72.1080

## 1. Introduction

Simple fluorocarbons have been received much interest not only in the semiconductor industry as a material of etching plasma but also in the field of electron collision physics as a prototype of polyatomic molecules. A considerable amount of experimental and theoretical efforts were reviewed by Christophorou *et al.*[1)] for $CF_4$, by Christophorou and Olthoff[2)] for $C_2F_6$, and by Christophorou and Olthoff[3)] for $C_3F_8$.

Among various electron scattering cross sections, the total electron scattering cross section (TCS, $\sigma_T$) is most fundamental which can be determined without any theoretical assumptions and serves as a normalization standard for the other electron scattering cross sections. Some dominant processes in the electron–molecule scattering may be seen from the behavior of $\sigma_T$ with respect to incident energy. It is hard to predict theoretically exact $\sigma_T$ values for polyatomic molecules. Therefore accurate measurement of $\sigma_T$ is important.

In Table I, listed are the absolute measurements of $\sigma_T$ for perfluorocarbons since 1986 together with the incident electron energy range and a type of the experimental technique. As shown in Table I, several groups used a TOF method for the measurement of $\sigma_T$. This technique has made possible to measure the inelastic cross sections at low energies. Although the linear transmission method is inferior to a TOF method in the energy resolution at low energies, this is still useful to obtain $\sigma_T$ over a wide energy range. There are two typical measurements whose method can be classified to the modified linear transmission. First, Szmytkowski *et al.*[5)] improved the energy resolution with a 127° electrostatic monochromator in the low and intermediate energy ranges. Second, Zecca *et al.*[6)] used a modified Ramsauer type apparatus for obtaining quasi monochromatic electrons at intermediate and high energy ranges. We have developed a compact linear type apparatus that can be applicable over a very wide energy range with a reasonable energy resolution.

Table I. List of measured $\sigma_T$ since 1986.

| Molecule | Author | Energy range (eV) | Experimental technique |
|---|---|---|---|
| $CF_4$ | Jones (1986) | 1–50 | TOF |
| | Szmytkowski (1992) | 0.45–200 | Linear, with 127° deflector |
| | Zecca (1992) | 75–4000 | Ramsauer |
| | Sueoka (1994) | 1–400 | TOF |
| $C_2F_6$ | Sanabia (1998) | 0–20 | TOF |
| | Szmytkowski (2000) | 0.5–250 | Linear, with 127° deflector |
| | Sueoka (2002) | 0.8–600 | TOF |
| $C_3F_8$ | Sanabia (1998) | 0–20 | TOF |
| | Tanaka (1999) | 0.8–600 | TOF |

At intermediate and high electron energy ranges, a major part of scattered electrons come through elastic or ionization processes. The total elastic electron scattering cross sections (integral elastic cross sections) $\sigma_{el}$ for molecules are basic quantities for electron–molecule collisions. Since the direct measurement of $\sigma_{el}$ for molecules is hard, we can estimate the values with $\sigma_T$ and the total ionization cross sections $\sigma_I$ in such energy range. In some cases, $\sigma_{el}$ for molecules were calculated by the Born approximation that is expected to be valid at high electron energy range. For understanding the electron–molecule collisions, it is desirable to measure $\sigma_T$ over a wide electron energy range.

Calibration of the electron energy scale is unavoidable in the electron scattering experiment especially at low energies. Szmytkowski *et al.*[5)] referred the vibrational resonant peaks of $N_2$. Sueoka *et al.*[7)] made the calibration by measuring the resonance profiles of $N_2$, CO and $CO_2$. In this study, the He resonance has been used as reference (shown later).

In the case of $\sigma_T$ measurements, the correction of electrons scattered into a forward narrow angular range (for brevity, ''forward scattered electrons'' will be used hereafter) is inevitable. Szmytkowski *et al.* and Zecca *et al.* estimated the contribution of the forward scattered electrons in their measured $\sigma_T$ values as 1% and 0.4%, respectively using available differential cross sections. Sueoka *et al.* also

*E-mail: nishimrh@kb3.so-net.ne.jp
†The deceased.
‡E-mail: nakamura@nkmr.elec.keio.ac.jp

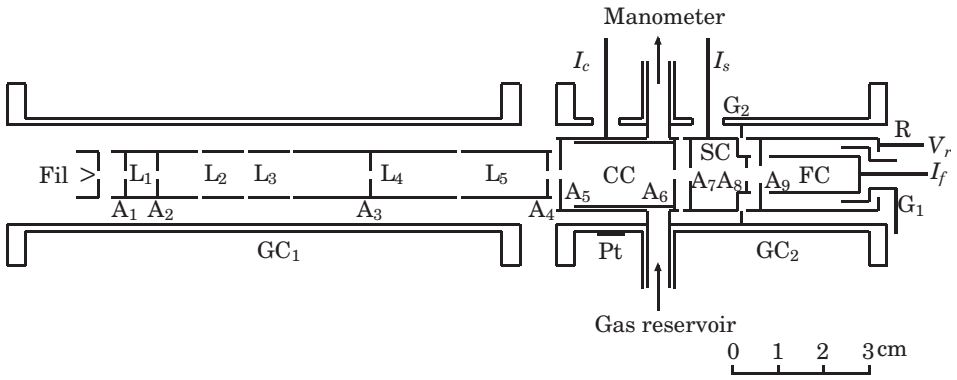


Fig. 1. Experimental apparatus.

corrected their results with available data of differential cross sections. In this study, the correction on this matter is explained in detail below in §2.2 Procedure.

## 2. Experimental

The apparatus used in this study is essentially the same as used in ref. 12 and shown schematically in Fig. 1. However some elements were renewed or introduced. Several modifications were made in the procedure for obtaining $\sigma_T$. Therefore the description of this section is given in some detail.

### *2.1 Apparatus*

A Pierce type electron gun with rhenium filament (hair pin type) and elements of electrostatic lens ($L_1$–$L_5$) are arranged in a guiding cylinder ($GC_1$). The collision cell (CC), the sub collision cell (SC) and a Faraday cup (FC) with a cylinder (R) for retarding potential are also arranged in a guiding cylinder ($GC_2$). The gun, each lens element and $GC_1$ are insulated from one another by circular disks of boron–nitride. The elements CC, SC, R, G1, FC and $GC_2$ are also isolated from one another by circular disks or thin rings made of polytetrafluoroethylene. All elements are assembled co-axially in a vacuum vessel which is evacuated below several $\times 10^{-5}$ Pa by a 6-inches oil diffusion pump with fluorinated oil and with liquid nitrogen trap. The earth's magnetic field around the apparatus is eliminated below several m gauss by a double coaxial mu-metal cylinder which is laid on the inside wall of the vacuum vessel (stainless steel 304L). A collimated electron beam ($\leq$300 pA) from the gun is introduced into CC, and SC through a thin molybdenum aperture (0.3 mm in thickness). Opening diameter of apertures $A_1$–$A_8$ are 0.5, 1.0, 1.0, 0.6, 1.0, 1.4, 1.8, and 2.4 mm, respectively. Opening diameter of $A_9$ is 5 mm. Material of all elements except filament of the gun and apertures $A_1$–$A_8$ is non-magnetic stainless steel (type 310). The gas pressure in CC is monitored with a capacitance manometer controlled at 45°C. During the measurement of $\sigma$, pressure of the vessel is kept below $3 \times 10^{-4}$ Pa.

#### *2.1.1 Sub-collision cell*

The drift cell used in ref. 12 is renewed as the sub-collision cell (SC). The role of SC is the same as earlier one: measurements of forward scattered electrons from the collision cell (CC) and of electrons scattered in SC. Only its shape was modified for the effective collection of transmitted electrons by the Faraday cup (FC).

#### *2.1.2 Electron collector*

The electron collector consists of three coaxial cylinders. As a retarding potential for incident electrons, a negative potential, which is equal to the electron acceleration voltage, is applied on the outer one (R). This cylinder also serves to prevent the emission of secondary electrons or the reflection of electrons from FC. The middle cylinder ($G_1$) is grounded for the suppression of leakage currents from R to FC. A grounded guard ring ($G_2$) is also inserted between SC and R for the same reason as for $G_1$.

#### *2.1.3 Thermometer*

For the observation of accurate temperature of a target gas in CC, a calibrated platinum thin-film device was attached on the outside of $GC_2$ instead of a thermister.[12)]

The assembly including SC and FC is shown schematically in Fig. 2.

### *2.2 Procedure*

In the case of a static gas target, an amount of the target gas effused from CC to the adjacent spaces should be estimated as accurate as possible. As discussed in an earlier work,[12)] the backward scattering of electrons from CC is negligible in this arrangement. Therefore a correction for the forward scattering of electron is considered. In the earlier work, the correction was estimated by repeated measurements of $\sigma_T$ for several different magunitude of the diameter of $A_6$.

In this study, the procedure is refined into more practical one. The total cross section $\sigma$ is defined by the Beer–Lambert relation as

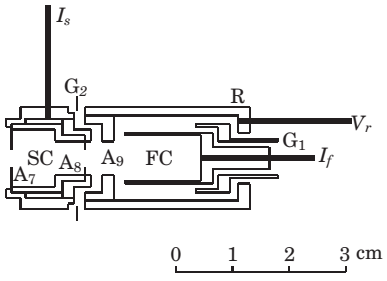


Fig. 2. Assembly of SC and FC.

$$I_f = I_0 \exp(-N\sigma l), \tag{2.1}$$

where $I_f$, $I_0$, $N$ and $l$ are the transmitted electron current, the incident electron current, the target gas number density and the electron scattering path length, respectively. Measurements are made for low (suffix 1) and high target gas pressures (suffix 2) successively. Equation (2.1) can be written as

$$\sigma = \frac{1}{l(N_2 - N_1)} \ln \frac{I_{02} I_{f1}}{I_{01} I_{f2}}. \tag{2.2}$$

Electrons scattered into very narrow forward angles in CC will pass through $A_6$ and $A_7$. A part of those electrons in CC and also in SC will pass through $A_8$. Those electrons are received as a part of $I_s$ or $I_f$. Therefore those electrons should be considered for the determination of $\sigma_T$.

### 2.2.1 *Determination of $\sigma_T$*

(1) Provisional cross section $\sigma_0$

For the determination of the provisional cross section $\sigma_0$, we regard the combined elements SC and FC as forming an electron collector. Then we can replace $I_f$, $I_0$ and $l$ in eq. (2.1) with $I_s + I_f$, $I_c + I_s + I_f$, and $l_0$, respectively. The provisional cross section $\sigma_0$ is determined as

$$I_s + I_f = (I_c + I_s + I_f) \exp(-N\sigma_0 l_0), \tag{2.3}$$

where $l_0 = 27.8$ mm is the geometrical length of CC. The currents $I_c$, $I_s$ and $I_f$ are received at CC, SC and FC, respectively.

(2) Improvement of the electron scattering path length

For the estimation of an effective electron scattering path length, an additional path length that is due to effusion of the target gas from CC to SC should be considered. For the discussion of the effused gas from CC to SC, we regard SC as a collision cell instead of CC. Then we can replace $I_0$ and $l$ in eq. (2.1) with $I_s + I_f$ and $\delta l$, respectively. Therefore the extended electron scattering path length $\delta l$ in SC is determined as

$$I_f = (I_s + I_f) \exp(-N\sigma_0 \delta l). \tag{2.4}$$

Although effusion of rarefied gas through an orifice must be independent of the electron energy, $\delta l$ indicates considerable dependence on the electron energy. In electron–simple molecule scattering, the intensity of electrons scattered in the forward narrow angle increase with increasing electron energy. The forward scattered electrons in CC and the scattered electrons in SC increase $I_s$ and, hence, increase $\delta l$. We can divide $\delta l$ into two parts: an energy independent part $\delta l_0$ and an energy dependent part $\delta l_1$.

$$\delta l = \delta l_0 + \delta l_1. \tag{2.5}$$

The first term $\delta l_0$ in eq. (2.5) gives the extended electron path length due to the effusion of a target gas from CC, which is determined as a minimum value in $\delta l$. The second term $\delta l_1$ gives the information about the forward scattered electrons in CC and the scattered electrons in SC. Therefore the improved electron scattering path length is given by

$$l = l_0 + \delta l_0. \tag{2.6}$$

(3) Temporal total cross section $\sigma_t$

Let us replace $l$ with $l_0 + \delta l_0$ in eq. (2.1), the temporal total cross section $\sigma_t$ is defined as

$$I_f = (I_c + I_s + I_f) \exp[-N\sigma_t (l_0 + \delta l_0)]. \tag{2.7}$$

The value $\sigma_t$ does not include the forward scattered electrons from CC to the adjacent spaces. Therefore further correction of $\sigma_t$ on this matter is indispensable for the determination of $\sigma_T$.

(4) Total cross section $\sigma_T$

The current $I_s$ in eq. (2.4) consist of electrons scattered in SC and forward scattered electrons in CC, which pass through $A_6$ and $A_7$. A part of forward scattered electrons in CC and SC also pass through $A_8$. Taking into account these two situations, the value $\sigma_0 \delta l$ in eq. (2.4) can be put approximately as

$$\sigma_0 \delta l = l_0 \delta\sigma - l_0 \delta\dot{\sigma} + \delta l_0 \sigma_0 - \delta l_0 \delta\ddot{\sigma}. \tag{2.8}$$

where $\delta\sigma$ is the cross section for forward scattered electrons in CC. Electrons scattered into such angular range will be received at the adjacent cell mostly and at FC finally. The second term $l_0 \delta\dot{\sigma}$ corresponds to the scattered electrons that will be received in FC. The third term is the usual scattered electrons in SC that is read out as $I_s$. The last term $\delta l_0 \delta\ddot{\sigma}$ is also the scattering cross section in the forward narrow angular range that is not measured in $I_s$ and must be added in $I_f$. Therefore negative sign is given for the second and the last term. Let the cross sections $\delta\sigma$ and $\delta\dot{\sigma}$ proportional to the solid angles viewing $A_7(\omega_1)$ and $A_8(\omega_2)$ from the electron path in CC, respectively. The ratio of the cross sections $(\delta\dot{\sigma}/\delta\sigma)$ is given as

$$\frac{\delta\dot{\sigma}}{\delta\sigma} = \frac{\int_0^{l_0} \omega_2 \mathrm{d}l}{\int_0^{l_0} \omega_1 \mathrm{d}l}. \tag{2.9}$$

Using the geometrical condition of each aperture set between $A_5$ and $A_8$ including $l_0 = 27.8$ mm, $\delta\dot{\sigma}/\delta\sigma = 0.08$ is given. Assuming $\delta\ddot{\sigma} = \delta\sigma$, the cross section $\delta\sigma$ is given from eqs. (2.5), (2.8) and (2.9) as

$$\delta\sigma = \frac{\sigma_0(\delta l - \delta l_0)}{l_0\left(1 - \dfrac{\delta\dot{\sigma}}{\delta\sigma}\right) - \delta l_0}. \tag{2.10}$$

In this apparatus, the lateral displacement of apertures $A_5$–$A_8$ from the central axis was designed within 0.1 mm. This is very small in comparison with a diameter of each aperture and gave no effect in the measured results essentially.

(5) Final correction of $\delta\sigma$.

However $\delta\sigma$ given by eq. (2.10) is not enough as a final correction term because this value is determined based on $\sigma_0$ that does not include the forward scattered electrons in CC. More realistically, $\sigma_0$ has to be replaced by $\sigma_0 + \delta\sigma$. A more plausible $\delta l^{(n+1)}$ is given as

$$\sigma_0 \delta l = \delta l^{(n+1)} (\sigma_0 + \delta\sigma^{(n)}) \tag{2.11}$$

where $\delta\sigma^{(0)} = \delta\sigma$. Replacing $\delta l$ in eq. (2.10) by $\delta l^{(n+1)}$, more plausible $\delta\sigma^{(n+1)}$ is given as

$$\delta\sigma^{(n+1)} = \frac{(\sigma_0 + \delta\sigma^{(n)})(\delta l^{(n+1)} - \delta l_0)}{l_0\left(1 - \dfrac{\delta\dot{\sigma}}{\delta\sigma}\right) - \delta l_0}. \tag{2.12}$$

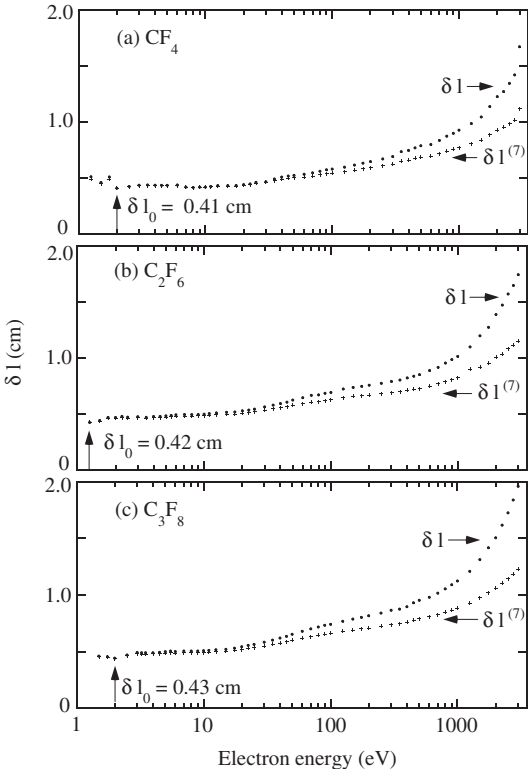


Fig. 3. $\delta l$ vs. incident electron energy.

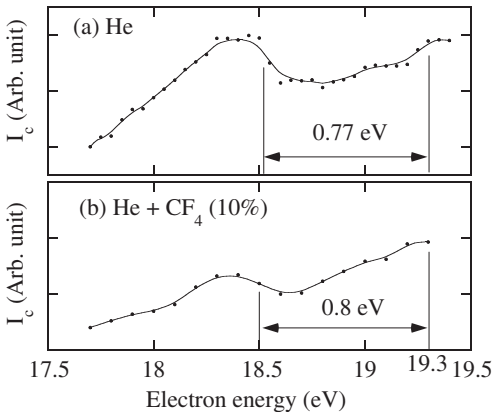


Fig. 4. He resonance in He and $CF_4$/He mixture.

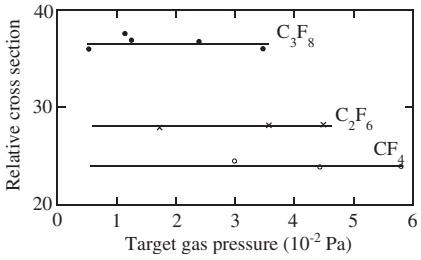


Fig. 5. $I_c$ vs. target gas pressure.

The value of $\delta\sigma^{(n+1)}$ is evaluated recurrently. In this study, the values for the three target molecules converged within 0.02% at $n = 6$. The total cross section $\sigma_T$ is given finally as

$$\sigma_T = \sigma_t + \delta\sigma^{(n+1)} \tag{2.13}$$

Figure 3 shows the behavior of $\delta l$ and $\delta l^{(7)}$ for all the target molecules as a function of incident electron energy.

### 2.2.2 *Electron energy calibration and energy width*

The kinetic energy of incident electrons in the collision volume CC is not equal to acceleration potentials applied on an electron source. This is due to the cumulative contact potential differences arose from many kind of metals used between the power supply and the electron source. For the estimation of the real electron energy in CC, $I_c$ including electrons scattered from an established resonance level in electron–atom collision is observed. First, $I_c$ was measured for pure He as a function of the electron acceleration potential applied to the electron source, which is shown in Fig. 4(a). In succession, a similar procedure was repeated for a target gas diluted with He. Figure 4(b) shows a profile of $I_c$ observed for $CF_4$ (10%) in He. As a location of the He 19.3 eV resonance appeared in the profile, we choose an energy that corresponds to a point of inflection on the observed profile. A resonance profile was seen at around 18.5 eV for He and perfluorocarbons diluted with He. For various concentrations of target gases in He, the profile of $I_c$ was observed at $18.50 \pm 0.05$ eV on the energy axis. Therefore we can conclude that electrons in CC are accelerated in excess of $0.80 \pm 0.05$ eV than an applied potential in this study.

Sharp profiles of the He 19.3 eV resonance were reported by Andrick and Ehrhardt.[13] A smoothed structure of the observed profile in this case may be attributed to a broad width of the energy of incident electrons which is estimated to be 0.25 eV (FWHM) from the observed profile.

### 2.2.3 *Pressure dependence of $\sigma_T$*

The dependence of $I_c$ on the target gas pressure is also examined for all the molecules at electron energies corresponding to these nearly at the maximum values of $\sigma_T$.

These results are shown in Fig. 5. Measurements were carried out in the pressure range where $\sigma_T$ is independent of the target gas pressure.

### 2.2.4 *Uncertainty*

Systematic uncertainties in the magnitudes of $\sigma_T$ values are introduced from the measurement of the electron currents, target gas pressures and electron path lengths. The purity of a target gas should be also considered as a source of the uncertainty. The uncertainties in the electron current and the target gas pressure are estimated to be 1.6% for each electrometer and 0.08% for the manometer, respectively. According to the supplier, a purity of the target gases is 99.95%. The uncertainty of the electron path length is estimated to be 3.6%. A voltmeter with the uncertainty of 0.002% used for the determination of the electron energy is allowed to operate within the range of $\leq$1 kV. For the measurement of the electron energies $E \geq 100$ eV, an active voltage attenuator with the uncertainty of 2.5% is attached in front of the voltmeter. The uncertainty of electron energy reading should be included as a part of the overall systematic uncertainty. Since at electron energies higher than 100 eV, the cross sections obtained in the present work showed a simple shape for all the gas targets, for the estimation of the uncertainty, we can fit $\sigma_T$ in a simple form only for convenience sake as

Table II. $\beta$ in eq. (2.14).

| Energy range (eV) | $\beta$ |
|---|---|
| 100–350 | 0.50 |
| 400–900 | 0.70 |
| 1000–3000 | 0.75 |

$$\sigma_T \propto E^{-\beta}, \tag{2.14}$$

where $\beta$ is dependent on the electron energy range as shown in Table II. The electron energy lower than 90 eV is measured with a voltmeter (uncertainty 0.002%) directly. Additionally, in the energy range between 10 eV and 50 eV, $\sigma_T$ does not change remarkably with respect to the electron energy. Therefore the contribution of the energy uncertaity 0.05 eV to the systematic uncertaity can be neglected in those energy ranges. In the energy range lower than 10 eV, the contribution of the uncertainty based on the electron energy to the systematic uncertainty is not considered since the electron beam has relatively broad energy width. The overall uncertainty is deduced from the root mean square sum of the systematic and the statistical uncertainty.

Table III. Total electron scattering cross sections for $CF_4$, $C_2F_6$ and $C_3F_8$ ($10^{-20}$ m$^2$) as a function of the electron energy $E$. Numbers in parentheses include both systematic and statistical uncertainties (%).

| $E$ (eV) | $CF_4$ | $C_2F_6$ | $C_3F_8$ |
|---|---|---|---|
| 1.25 | 9.61(4.8) | 15.4(4.7) | |
| 1.5 | 9.60(4.7) | 16.2(4.4) | 21.1(4.8) |
| 1.75 | 10.2(4.7) | 16.8(4.5) | 22.3(4.4) |
| 2.0 | 10.4(4.5) | 17.2(4.4) | 23.0(4.5) |
| 2.25 | | 17.3(4.3) | |
| 2.5 | 11.0(4.3) | 17.6(4.3) | 28.0(4.4) |
| 3.0 | 11.8(4.4) | 18.5(4.3) | 33.1(4.3) |
| 3.25 | | | 34.9(4.4) |
| 3.5 | 12.5(4.3) | 20.9(4.4) | 35.9(4.3) |
| 4.0 | 12.8(4.3) | 24.1(4.3) | 35.7(4.3) |
| 4.5 | 13.0(4.3) | 26.4(4.3) | 34.8(4.3) |
| 5.0 | 13.3(4.3) | 27.6(4.3) | 34.6(4.3) |
| 5.5 | | 27.4(4.3) | 35.8(4.3) |
| 6.0 | 14.4(4.3) | 26.9(4.3) | 37.1(4.3) |
| 7.0 | 17.3(4.3) | 27.6(4.3) | 37.7(4.3) |
| 8.0 | 19.7(4.3) | 28.8(4.3) | 38.8(4.3) |
| 9.0 | 20.4(4.2) | 29.7(4.4) | 39.0(4.3) |
| 10 | 19.5(4.3) | 28.9(4.3) | 37.7(4.3) |
| 11 | 18.3(4.3) | 27.5(4.3) | 35.6(4.3) |
| 12.5 | 17.3(4.3) | 26.2(4.3) | 33.9(4.3) |
| 15 | 17.2(4.3) | 26.2(4.3) | 33.9(4.3) |
| 17.5 | 17.5(4.3) | 27.2(4.3) | 35.2(4.3) |
| 20 | 18.2(4.3) | 28.9(4.3) | 37.3(4.3) |
| 22.5 | 19.2(4.3) | 29.9(4.3) | 38.6(4.3) |
| 25 | 19.4(4.3) | 30.4(4.3) | 39.3(4.3) |
| 30 | 19.8(4.3) | 31.3(4.3) | 40.3(4.3) |
| 35 | 19.6(4.3) | 31.5(4.3) | 41.1(4.3) |
| 40 | 19.7(4.3) | 31.7(4.3) | 41.4(4.3) |
| 45 | 20.1(4.3) | 31.7(4.3) | 41.4(4.3) |
| 50 | 20.5(4.3) | 31.7(4.3) | 41.1(4.3) |
| 60 | 20.3(4.3) | 31.3(4.3) | 41.2(4.3) |

## 3. Results and Discussion

The measured results are shown in Tables III and IV together with the total uncertainty. Results for each molecule are compared with available experimental and theoretical data in the following subsections.

### *3.1 $CF_4$*

Figure 3(a) shows the behavior of $\delta l$ in SC. From the minimum value of $\delta l$ at 2 eV, the effective electron scattering path length in SC is $\delta l_0 = 0.41$ cm.

In Fig. 6(a), the present results for $CF_4$ are shown together with available experimental and theoretical data since 1986. A prominent broad peak at 8–9 eV and three small shoulders at 2 eV, at 4 eV, at 22.5 eV can be seen. Boesten *et al.*[20] carried out the beam experiment and concluded that a main contribution to the first peak is the shape resonance due to the temporal electron trapping in the unoccupied C–F orbital with many vibrational excitation modes (mainly $\nu_3$). Szmytkowski *et al.*[5] explained the broad hump at around 25 eV as a pile of weak resonant and direct processes. From the results of Boesten *et al.* the first shoulder at 2 eV can be attributed to the excitation of the $\nu_3$ mode.

The agreement between the present results and those of Jones[4] is good. The present results agree well with those of Szmytkowski *et al.*[5] in the energy range overlapped with each other. The results of Sueoka *et al.*[7] agree very well

Table IV. Total electron scattering cross sections for $CF_4$, $C_2F_6$ and $C_3F_8$ ($10^{-20}$ m$^2$) as a function of the electron energy $E$. Numbers in parentheses include both systematic and statistical uncertainties (%).

| $E$ (eV) | $CF_4$ | $C_2F_6$ | $C_3F_8$ |
|---|---|---|---|
| 70 | 19.6(4.3) | 30.1(4.3) | 39.8(4.4) |
| 80 | 18.7(4.3) | 29.5(4.3) | 38.2(4.4) |
| 90 | 18.2(4.3) | 28.4(4.4) | 37.4(4.4) |
| 100 | 17.5(4.4) | 27.4(4.7) | 35.8(4.4) |
| 125 | 16.1(4.4) | 25.0(4.5) | 33.7(4.5) |
| 150 | 14.9(4.5) | 23.4(4.5) | 31.4(4.5) |
| 175 | 13.9(4.5) | 22.2(4.6) | 29.7(4.5) |
| 200 | 13.0(4.5) | 20.7(4.5) | 27.9(4.6) |
| 250 | 11.5(4.5) | 18.5(4.5) | 24.7(4.6) |
| 300 | 10.4(4.5) | 16.5(4.5) | 22.7(4.6) |
| 350 | 9.60(4.5) | 15.2(4.6) | 20.7(4.6) |
| 400 | 8.83(4.7) | 13.9(4.8) | 18.7(4.8) |
| 450 | 8.26(4.7) | 12.9(4.8) | 17.7(4.8) |
| 500 | 7.74(4.7) | 12.1(4.8) | 16.6(4.8) |
| 600 | 6.77(4.7) | 10.6(4.8) | 14.7(4.8) |
| 700 | 6.09(4.7) | 9.50(4.8) | 13.1(4.9) |
| 800 | 5.48(4.8) | 8.78(4.8) | 11.9(4.9) |
| 900 | 5.02(4.8) | 7.96(4.8) | 11.0(4.9) |
| 1000 | 4.63(4.8) | 7.42(4.9) | 10.1(5.0) |
| 1250 | 3.87(4.9) | 6.21(4.9) | 8.54(5.0) |
| 1500 | 3.35(4.9) | 5.38(5.0) | 7.54(5.1) |
| 1750 | 3.01(5.0) | 4.76(5.1) | 6.78(5.1) |
| 2000 | 2.69(5.1) | 4.30(5.1) | 6.16(5.2) |
| 2250 | 2.42(5.1) | 4.00(5.2) | 5.72(5.3) |
| 2500 | 2.22(5.1) | 3.75(5.2) | 5.32(5.3) |
| 2750 | 2.06(5.2) | 3.52(5.3) | 5.03(5.4) |
| 3000 | 2.00(5.4) | 3.31(5.3) | 4.76(5.4) |

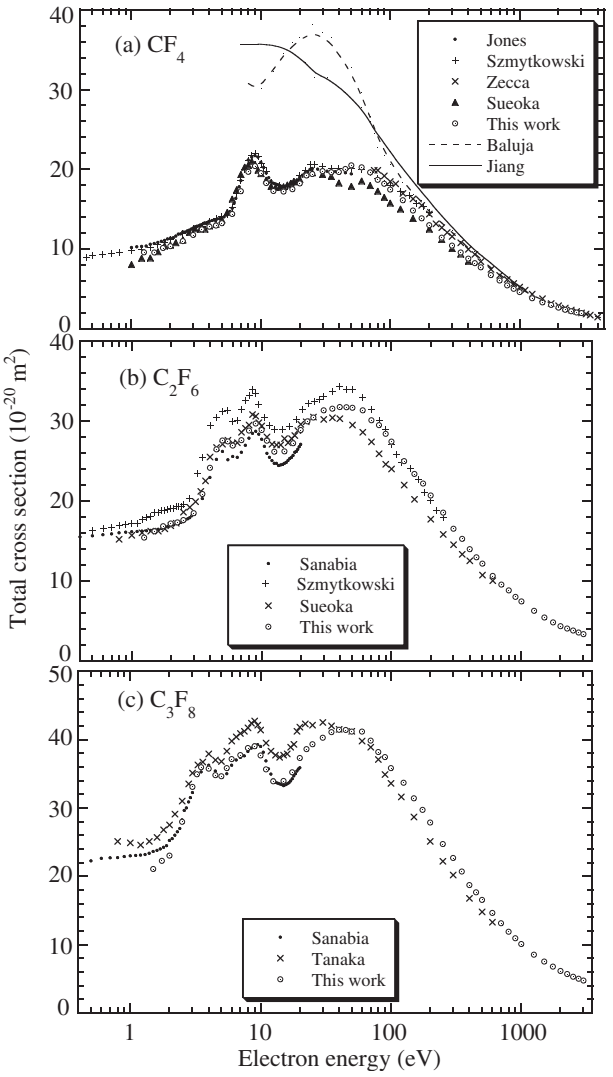


Fig. 6. $\sigma_T$ vs. electron energy.

with ours in the energy range lower than 25 eV, while their results are considerably lower than the present results in the energy range between 30 eV and 100 eV. Results of Zecca *et al.*[6] agree very well with ours. Calculated results of Baluja *et al.*[16] agree well with the present results at energies above 800 eV. The discrepancy between the theoretical results of Jiang *et al.*[17] and ours decreases with increasing electron energy.

### 3.2 $C_2F_6$

Figure 3(b) shows the behavior of $\delta l$ in SC. From the minimum value at 1.25 eV, the effective electron path length in SC is selected as $\delta l_0 = 0.42$ cm.

In Fig. 6(b), the present results for $C_2F_6$ are shown along with those of Sanabia *et al.*,[8] Szmytkowski *et al.*[9] and Sueoka *et al.*[10] A small hump and distinct two peaks can be seen at energies of 2–2.25 eV, 4–5 eV and 8–9 eV, respectively. Takagi *et al.*[21] concluded from their beam experiment that the first hump is the direct excitation of the vibrational $\nu_s$ mode (stretching, mainly $\nu_1$), the second and the third peaks are the vibrational resonant excitation of many $\nu_s$ and partly bending modes $\nu_b$. They also concluded the cause of the third one at 8–9 eV is the same mechanism as in the case of $CF_4$.

Agreement between this work and those of Sanabia *et al.*[8] is good at energies between 2.25 eV and 5 eV, while their results are lower than ours at higher energies up to about 7%. Measured results of Szmytkowski *et al.*[9] are higher than ours in the energy range between 3 eV and 70 eV, and agree very well with ours at energies above 80 eV. Results of Sueoka *et al.*[10] agree very well with ours at energies below 25 eV, while notable differences between the two are seen at energies higher than 30 eV.

### 3.3 $C_3F_8$

Figure 3(c) shows the behavior of $\delta l$ in SC. From the minimum value at 2 eV, the effective electron path length in SC is determined as $\delta l_0 = 0.43$ cm.

In Fig. 6(c), the present results for $C_3F_8$ are shown along with those of Sanabia *et al.*[8] and Tanaka *et al.*[11] Two distinct peaks at 3–4 eV and 8–9 eV, and two slight shoulders at 6 eV and 22.5 eV can be seen. Tanaka *et al.*[11] concluded from their crossed beam experiment that those are due to shape resonance related to the temporal negative ion formation in some C–F unoccupied orbitals. Although a resonance peak at 8–9 eV appeared in $\sigma_T$ of those three targets commonly, an extra distinct peak was excited at 4–5 eV for $C_2F_6$ and 3–4 eV for $C_3F_8$. Agreement between the results of Sanabia *et al.* and ours is very good except at energies below 2 eV. The results of Tanaka *et al.* are higher than ours at energies below 30 eV and lower at energies above 60 eV. They also reported a broad peak at 20–30 eV, while ours did not show such a clear structure in those energy range. However these three experimental results agree very well with each other in the relative shape of $\sigma_T$ in the energy range lower than 20 eV.

### 3.4 *Elastic cross section*

The difference between $\sigma_T$ and $\sigma_I$ is approximately equal to elastic cross sections $\sigma_{el}$ at high energies if inelastic processes other than ionization can be ignored. Previously one of authors (H.N.) reported the gross total ionization cross sections $\sigma_I$ of $CF_4$, $C_2F_6$ and $C_3F_8$.[18] Figures 7(a), 7(b), 7(c) show the difference between the present results $\sigma_T$ and those of $\sigma_I$[18] for these molecules at energies higher than 20 eV. Available elastic cross sections are also shown in these figures. As can be seen in Fig. 7, agreement among this work, Sakae *et al.*[19] and Balija *et al.*[16] is very good. On the other hand the results of Boesten *et al.*[20] for $CF_4$, Takagi *et al.*[21] for $C_2F_6$ and Tanaka *et al.*[11] for $C_3F_8$ are a little bit smaller than ours at energies higher than 50 eV, which may suggest the upper bound of inelastic cross sections other than ionization processes.

Reliable elastic scattering cross section values are of importance not only for the normalization of the excitation cross sections but also for a validity test of the theoretical approximation. For more detailed discussion, extended theoretical and experimental studies on the elastic scattering are needed.

## 4. Concluding Remarks

A set of $\sigma_T$ for simple perfluorocarbons was measured over a wide energy range using a compact linear transmission apparatus. Data at high energies for $C_2F_6$ and $C_3F_8$ were given. Forward scattered electrons from CC were

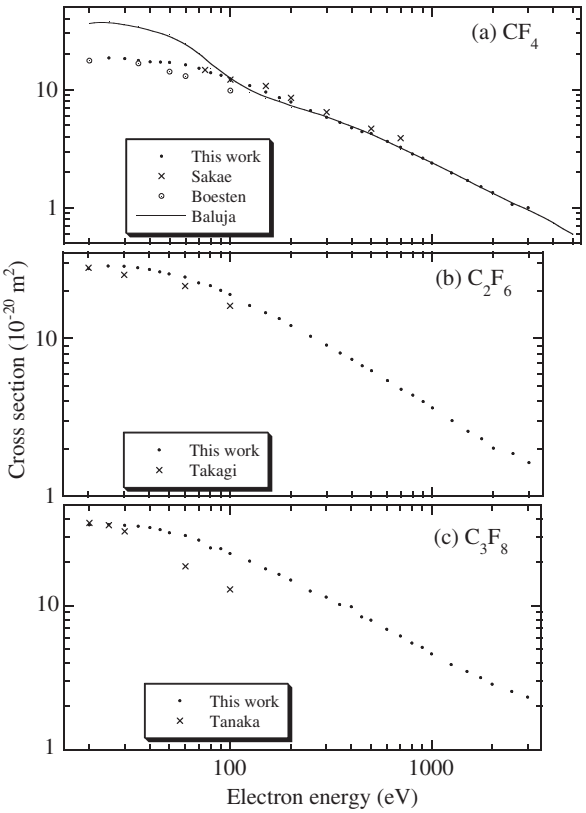


Fig. 7. $\sigma_T$–$\sigma_I$ and $\sigma_{el}$ vs. electron energy.

corrected in the experimental procedure. The correction of $\sigma_T$ corresponding to the forward scattered electrons is conspicuous at high electron energy range especially in the case of a compact experimental apparatus. For example, the correction rates $\delta\sigma^{(7)}/\sigma_T$ at 3 keV were 26%, 27% and 29% for $CF_4$, $C_2F_6$ and $C_3F_8$, respectively. Excellent agreement among the present results and available data can be seen at energies lower than 10 eV and at higher than about 1 keV for $CF_4$. On the other hand, considerable discrepancy can be seen among the available data for $C_2F_6$ and for $C_3F_8$ at low energies. Upper bound of $\sigma_{el}$ was also estimated for all molecules studied and compared with available data.

## Acknowledgments

This work was partly supported by the cooperative program of the National Institute for Fusion Science. Authors thank helpful discussion with Professor O. Sueoka. They express their gratitude to Professor Y. Hatano for his valuable comments. They also wish to thank Professor K. Takayanagi for his helpful discussions and advices.

1) L. G. Christophorou, J. K. Olthoff and M. V. V. S. Rao: J. Phys. Chem. Ref. Data **25** (1996) 1341.
2) L. G. Christophorou and J. K. Olthoff: J. Phys. Chem. Ref. Data **27** (1998) 1.
3) L. G. Christophorou and J. K. Olthoff: J. Phys. Chem. Ref. Data **27** (1998) 889.
4) R. Jones: J. Chem. Phys. **84** (1986) 813.
5) Cz. Szmytkowski, A. M. Krzysztofowicz, P. Janicki and L. Rosenthal: Chem. Phys. Lett. **199** (1992) 191.
6) A. Zecca, G. P. Karwasz and R. S. Brusa: Phys. Rev. A **46** (1992) 3877.
7) O. Sueoka, S. Mori and A. Hamada: J. Phys. B **27** (1994) 1453.
8) J. E. Sanabia, G. D. Cooper, J. A. Tossel and H. Moore: J. Chem. Phys. **108** (1998) 389.
9) Cz. Szmytkowski, P. Mozejko, G. Kasperski and E. Ptasinska-Denga: J. Phys. B **33** (2000) 15.
10) O. Sueoka, C. Makochekanwa and H. Kawate: Nucl. Instrum. Methods B **192** (2002) 206.
11) H. Tanaka, Y. Tachibana, M. Kitajima, O. Sueoka, H. Takaki, A. Hamada and M. Kimura: Phys. Rev. A **59** (1999) 2006.
12) H. Nishimura and T. Sakae: Jpn. J. Appl. Phys. **29** (1990) 1372.
13) D. Andrick and H. Ehrhardt: Z. Phys. **192** (1966) 99.
14) A. Zecca, I. Lazzizzera and R. S. Brusa: Phys. Rev. A **45** (1992) 2777.
15) A. Zecca, G. P. Karwasz and R. S. Brusa: Phys. Rev. A **46** (1992) 3877.
16) K. L. Baluja, A. Jain, V. Di. Martino and F. A. Giantuco: Europhys. Lett. **17** (1992) 139.
17) Y. Jiang, J. Sun and L. Wan: Phys. Rev. A **52** (1995) 398.
18) H. Nishimura, W. M. Huo, M. A. Ali and Y.-K. Kim: J. Chem. Phys. **110** (1999) 3811.
19) T. Sakae, S. Sumiyoshi, E. Murakami, Y. Matsumoto, K. Ishibashi and A. Katase: J. Phys. B **22** (1989) 1385.
20) L. Boesten, H. Tanaka, A. Kobayashi, M. A. Dillom and M. Kimura: J. Phys. B **25** (1992) 1607.
21) T. Takagi, L. Boesten, H. Tanaka and M. A. Dillon: J. Phys. B **27** (1994) 5389.